

Aggregation methods in food chains with nutrient recycling

B.W. Kooi^{a*}, J.C. Poggiale^b,
P. Auger^c, S.A.L.M. Kooijman^a

^a Faculty of Biology, Institute of Ecological Science, Vrije Universiteit,
De Boelelaan 1087, 1081 HV Amsterdam, The Netherlands

^b Centre D'Océanologie de Marseille, U.M.R. 6535,
Campus de Luminy Case 901, 13288 Marseille Cedex 9, France

^c Université Claude Bernard, Lyon 1, UMR CNRS 5558,
43 Bd du 11 Novembre 1918, 69622 Villeurbanne Cedex, France

Abstract

This paper is devoted to the study of food chain models under batch and chemostat conditions where nutrient recycling is taken into account. The food chain is formed by a nutrient and two populations, prey and predator (producers and consumers). Species at both trophic levels digest their food source only partly. The unusable parts of the food not used for growth is ejected in the reactor as faeces together with metabolic products. The excreted material together with death material, detritus, is decomposed and this gives the recycling of the nutrient. In closed (batch-type environment) systems the elemental matter needed by producers must be provided through recycling where light energy from the environment supplies the necessary energy that fuels the life processes. In open (chemostat-type environment) systems this energy is added to the system via the chemical energy stored in the organic compounds in the inflow. An aggregation method is developed for situations in which each trophic level is characterized by differing time scales. This allows us to reduce the dimension of the model which gives good approximations after the fast transient. We will show that in the chemostat case first-order approximations are needed in order to get the same qualitative long-term dynamics for both the full and the reduced model.

Keywords: Aggregation methods, Batch reactor, Chemostat, Food chains, Nutrient recycling.

*Corresponding author. E-mail: kooi@bio.vu.nl, Tel: +31 (0)20 4447129, Fax: +31 (0)20 4447123

1 Introduction

We study the effects of material recycling on the long-term dynamic behaviour of a simple food web. Recently it is found that effects of nutrient recycling plays an important role to the stability of ecosystems (DeAngelis, 1992). With nutrient recycling, waste-products and dead organisms from the biotic trophic levels are mineralised, possibly by a decomposer, into the abiotic nutrient. In the literature closed (batch-type environment) and open (chemostat-type environment) ecosystems are analysed.

In a batch reactor system the biological components and the nutrient are added to a closed system and thereafter the system is self-sustaining. In (Nisbet and Gurney, 1976) an elucidating model for carbon cycling in a closed ecosystem is described. In that model respiration products are converted directly to inorganic material, carbon dioxide CO_2 , at a fixed rate proportional to the biomass of the population. This implies the assumption that the presence of decomposers does not significantly influence the rate of provision of material for decomposition and that decomposition is sufficiently fast to neglect time delays in the decomposition process. Two types (dissolved and particulate) of nutrients are distinguished in (Aota and Nakajima, 2000) where they study coexistence of phytoplankton and bacteria with nutrient recycling in a close ecosystem. Phytoplankton can use only dissolved (inorganic) nutrients while the bacteria degrade particulate nutrient (dead bodies of phytoplankton and bacteria) as well. In (Kooijman and Nisbet, 2000) the complete mass and energy turnover in a daphnids–algae–bacteria (consumers–producers–decomposers) community in a closed bottle is evaluated. The daphnids consume both algae and bacteria. The algae use solar energy to convert carbon dioxide CO_2 to organic compounds. Different model formulations for the consumers were considered. Bacteria, the decomposers, digest their faeces and those of the algae, and dead *Daphnia*, both instantaneously and completely.

In a chemostat there is a continuous flow of the nutrient through the reactor containing the populations. Chemostat conditions might resemble some ecosystems in a very simple model for a lake of other aquatic habitats, see also (DeAngelis, 1992). In (Beretta *et al.*, 1990; Ruan, 1993; Ruan, 2001) a distributed time lag in the recycling is introduced to model time required to regeneration of nutrient from dead biomass by bacterial decomposition whereby the dynamics of the decomposer is not modelled.

The production of degradable material at each trophic level occurs as side effects of three biological processes. These three processes involved in the living of each population are the assimilation, maintenance and growth process, (Kooijman, 2000). Only a part of the food ingested by species is assimilated and the unusable parts are ejected in the reactor in the form of faeces. Subsequently, a part of the assimilated material is used for synthesis of new biomass and the other part forms metabolic products associated with the maintenance and the growth process, that are excreted in the reactor. With our model formulation products are formed at two rates as waste-products by the three processes. One product is formed at a rate proportional to the biomass, modelling metabolic waste-products which are assumed to be degraded instantaneously into nutrients. We neglect formation of death material which would be also proportional to biomass. Another product is formed at a rate

proportional to the ingestion rate modelling the production of faeces which are degraded exponentially a fixed recycle rate. This yields extra state variables for each trophic level. Remark that the decomposers are not modelled explicitly.

One of our objective is to obtain a better insight in the dynamical properties of the system by reducing the dimension. We use aggregation methods for this purpose. With perfect aggregation new global variables are defined which allows one to describe the dynamics of the system in a condensed way (Iwasa *et al.*, 1987; Iwasa *et al.*, 1989). In previous papers, we used perturbation techniques to perform approximate aggregation which have been applied to complex ecological models with different time scales (Auger *et al.*, 2000a). The method works when the fast system possesses a stable equilibrium (Auger and Poggiale, 1996) and also with a stable limit cycle (Poggiale and Auger, 1996). Here we shall take advantage of the different time scales for the trophic levels of the food chain to apply aggregation methods, singular perturbation techniques, to simplify the models for the dynamics of the system.

In (Rinaldi and Muratori, 1992a; Rinaldi and Muratori, 1992b; Muratori and Rinaldi, 1989; Muratori and Rinaldi, 1992) a singular perturbation technique is applied to slow-fast systems. The model is the Rosenzweig-MacArthur model where the lowest trophic level grows logistically when not predated, that is nutrients are not modelled explicitly; they determine implicitly the carrying capacity. The trophic interactions are modelled using the Holling type II functional response. Different time-scales for the trophic levels is obtained by assuming a low efficiency for the trophic levels, that is, the maximum growth rate of each population is a small fraction of its maximum ingestion rate.

Since we study the effects of nutrient recycling we use a mass-balance model where the nutrients are modelled explicitly. We assume here complete recycling of the nutrients in the food chain. This facilitates the use of mass conservation laws with the formulation of the model. In (Kooi *et al.*, 1998), we applied aggregation methods to bi-trophic food chains under two environmental conditions, batch and chemostat, where the batch condition is a special case of the chemostat condition with dilution rate equal zero. The model was a mass-balance model where nutrients are modelled explicitly. We assumed different time scales for the trophic levels, but we kept the efficiencies at their normal magnitude. As a consequence, there is no complete time scale separation. The model analysed in (Kooi *et al.*, 1998) is a special case of the model analysed here with no maintenance and zero recycle rates of the faeces and metabolic products.

Under chemostat conditions the reduced system has a stable equilibrium while the full model possesses a stable limit cycle when the nutrient is abundant. We will show that first-order approximations are needed for getting oscillating long-term dynamics for both the full and the reduced system. Then, the reduced system has two slow manifolds and the trajectory follows one slow manifold. When this manifold becomes unstable, the trajectory jumps to the other manifold. The trajectory continues to move along this manifold until it becomes unstable and the trajectory jumps back to the first manifold, and so on and this forms a quasi-limit cycle.

2 Model description

In this section we give the model for a predator–prey–nutrient system in a closed or open environment with nutrient recycling. Thereafter the relationship with models proposed and analysed in the literature is described.

Every food web being a closed system is based on producers that convert carbon dioxide CO₂ to organic compounds. This process is carried out predominately by photosynthetic organisms that convert light energy to chemical energy; the chemical energy is stored within the organic compounds that are formed. These autotrophic organisms are plants in terrestrial systems and photosynthetic organisms such as the algae in marine systems. Most algae have also heterotrophic capabilities to supplement their energy and nutrient requirement and are called mixotrophs. The produced organic carbon becomes available to heterotrophic consumers. Hence, in closed systems, with no exchange of matter with the environment, energy is supplied to the system as light energy (solar radiation), otherwise the community will dissipate the available energy since biological processes are dissipative by the generation of waste heat, and therefore the community disappears. The waste heat leaves the system by convection or radiation.

In open systems consisting of heterotrophic organisms there is an input of allochthonous organic matter and chemical energy at the same time. There is no inflow of light energy, but there is loss of energy via chemical energy in the matter that leaves the system and via convection or radiation of waste heat. When an autotroph or mixotroph is part of the food chain in an open system, light energy is supplied besides the chemical energy of the input matter.

We assume that the reactor is spatially homogeneous and with a time-invariant input of the nutrient while all community components are washed-out at possibly different rates. We denote the nutrient concentration by x_0 , prey biomass by x_1 and predator biomass by x_2 . The produced degradable materials excreted by the prey population are denoted by p_1 and z_1 and those produced by the predator population by p_2 and z_2 . The model with nutrient recycling, reads

$$\frac{dx_0}{d\tau} = (x_r - x_0)D_0 - I_{0,1}f_{0,1}(x_0)x_1 + \alpha_1p_1 + \beta_1z_1 + \alpha_2p_2 + \beta_2z_2 , \quad (1a)$$

$$\frac{dx_1}{d\tau} = \mu_{0,1}f_{0,1}(x_0)x_1 - m_1x_1 - D_1x_1 - I_{1,2}f_{1,2}(x_1)x_2 , \quad (1b)$$

$$\frac{dx_2}{d\tau} = \mu_{1,2}x_2f_{1,2}(x_1) - m_2x_2 - D_2x_2 , \quad (1c)$$

$$\frac{dp_1}{d\tau} = ((I_{0,1} - \mu_{0,1})f_{0,1}(x_0)x_1 - \alpha_1p_1) - D_1p_1 , \quad (1d)$$

$$\frac{dp_2}{d\tau} = ((I_{1,2} - \mu_{1,2})f_{1,2}(x_1)x_2 - \alpha_2p_2) - D_2p_2 , \quad (1e)$$

$$\frac{dz_1}{d\tau} = m_1x_1 - \beta_1z_1 - D_1z_1 , \quad (1f)$$

$$\frac{dz_2}{d\tau} = m_2x_2 - \beta_2z_2 - D_2z_2 , \quad (1g)$$

where $f_{i-1,i}(x_{i-1})$ are the scaled Holling type II functional responses for $i = 1, 2$ defined by

$$f_{i-1,i}(x_{i-1}) = \frac{x_{i-1}}{k_{i-1,i} + x_{i-1}} . \quad (2)$$

In Figure 1 the material fluxes through the food chain are depicted. The equations given above are derived by applying mass conservation laws for each compartment indicated in Figure 1. See Table 2 for a definition of the parameters. For biologically realistic situations some of the parameters are related as follows: $I_{i-1,i} > \mu_{i-1,i} > 0$ and $0 \leq m_i < \mu_{i-1,i}$ while $\mu_{1,2} < \mu_{0,1}$.

The three processes involved in the living of each population are the assimilation, maintenance and growth process. The formation rate of faeces $(I_{i-1,i} - \mu_{i-1,i})f_{i-1,i}(x_{i-1})x_i$ is the ingestion rate minus the growth rate times the biomass of the population. The formation rate of the metabolic products $m_i x_i$ is proportional to the biomass of the population. The decomposers are not modelled explicitly but the materials released by the species in the reactor are degraded exponentially into nutrients, the terms $\alpha_i p_i$ and $\beta_i z_i$.

Some terms in system (1) may have different biological interpretations. For instance, m_i , $i = 1, 2$ are often called respiration rate constants and the D_i 's are removal rates possibly due to natural death or wash-out.

The two environmental conditions considered in this paper are the batch reactor and the chemostat reactor. When $D_i = 0$, $i = 0, 1, 2$ there is no input of nutrients at the basis of the food chain nor output at all trophic levels. This describes the batch reactor. For this closed system no mass is exchanged with the environment. On the other hand, when $D_i = D$, $i = 0, 1, 2$, the equations describe the dynamics of a food chain in a chemostat reactor where $D > 0$ is the dilution rate and $x_r > 0$ the concentration of the nutrient in the reservoir.

In this model formulation instantaneous recycling of the respiratory products and the faeces is obtained by assuming a fast nutrient recycling rate, that is $\alpha_i \gg \mu_{i-1,i}$ and $\beta_i \gg \mu_{i-1,i} > m_i$. Then, the last four equations (1d–1g) give

$$\alpha_1 p_1 = (I_{0,1} - \mu_{0,1}) f_{0,1}(x_0) x_1 , \quad (3a)$$

$$\alpha_2 p_2 = (I_{1,2} - \mu_{1,2}) f_{1,2}(x_1) x_2 , \quad (3b)$$

$$\beta_1 z_1 = m_1 x_1 , \quad (3c)$$

$$\beta_2 z_2 = m_2 x_2 , \quad (3d)$$

where we used that D_i are negligible small with respect to α_i and β_i for $i = 1, 2$. These expressions must be substituted in (1a) which together with (1b) and (1c) forms an reduced model for the predator-prey system in the chemostat. Here we will assume that $\beta_i = \infty$, $i = 1, 2$, that is instantaneous degradation of the labile maintenance-associated products and we neglect natural death. We take $0 < \alpha_i < \infty$, that is the particulate nutrients are regenerated by bacteria which are assumed to be available *ad libitum*, so that we do not model their dynamics explicitly. Notice that when $\alpha_i = \beta_i = 0$, $i = 1, 2$ the model boils down to the predator-prey model without recycling analysed in (Kooi *et al.*, 1998).

In (Ruan, 1993; Ruan, 2001) a model is described and analysed for a zooplankton-phytoplankton-nutrient (consumer–producer–nutrient) system where the zooplankton as well as the phytoplankton consume nutrients. In that formulation no additional state variables are introduced for the respiratory products nor faeces, but the zooplankton is recycled instantaneous similar to the conditions (3). There is a term similar to the metabolic product term, but the biological interpretation is solely physiological death and not due to metabolic respiration.

In (Ruan, 1993) the phytoplankton and the zooplankton die with species specific rates and are recycled at a possible different nutrient recycle rate

$$\begin{aligned} \frac{dx_0}{d\tau} = & (x_r - x_0)D - I_{0,1}f_{0,1}(x_0)x_1 + \gamma_1 m_1 x_1 + \gamma_2 m_2 x_2 + \\ & (I_{0,1} - \mu_{0,1})f_{0,1}(x_0)x_1 + (I_{1,2} - \mu_{1,2})f_{1,2}(x_1)x_2 , \end{aligned} \quad (4a)$$

$$\frac{dx_1}{d\tau} = \mu_{0,1}f_{0,1}(x_0)x_1 - m_1 x_1 - D x_1 - I_{1,2}f_{1,2}(x_1)x_2 , \quad (4b)$$

$$\frac{dx_2}{d\tau} = \mu_{1,2}x_2 f_{1,2}(x_1) - m_2 x_2 - D x_2 , \quad (4c)$$

where $\gamma_i < 1$ indicating that only a part of the dead material is recycled. This model, which is system (1) where (3) is taken into account, is a straightforward extension of the phytoplankton–nutrient model analysed in (Beretta *et al.*, 1990). In (Ruan, 2001) the plankton model (4) was extended with delayed nutrient recycling. In our notations equation (4a) becomes

$$\begin{aligned} \frac{dx_0}{d\tau} = & (x_r - x_0)D - I_{0,1}f_{0,1}(x_0)x_1 + \gamma_1 \int_{-\infty}^t F(t-s)x_1(s) ds + \gamma_2 \int_{-\infty}^t G(t-s)x_2(s) ds + \\ & (I_{0,1} - \mu_{0,1})f_{0,1}(x_0)x_1 + (I_{1,2} - \mu_{1,2})f_{1,2}(x_1)x_2 . \end{aligned}$$

The instantaneous recycling of model (4) is obtained by assuming $F(s) = G(s) = \delta(s)$, where δ is the Dirac delta function.

In the next section we will use aggregation techniques to derive reduced systems of the following full system where ε enforces time-separation

$$\frac{dx_0}{d\tau} = (x_r - x_0)D_0 - I_{0,1}f_{0,1}(x_0)x_1 + \alpha_1 p_1 + m_1 x_1 + \alpha_2 p_2 + \varepsilon m_2 x_2 , \quad (5a)$$

$$\frac{dx_1}{d\tau} = \mu_{0,1}f_{0,1}(x_0)x_1 - m_1 x_1 - D_1 x_1 - \varepsilon I_{1,2}f_{1,2}(x_1)x_2 , \quad (5b)$$

$$\frac{dx_2}{d\tau} = \varepsilon (\mu_{1,2}x_2 f_{1,2}(x_1) - m_2 x_2) - D_2 x_2 , \quad (5c)$$

$$\frac{dp_1}{d\tau} = (I_{0,1} - \mu_{0,1})f_{0,1}(x_0)x_1 - \alpha_1 p_1 - D_1 p_1 , \quad (5d)$$

$$\frac{dp_2}{d\tau} = \varepsilon (I_{1,2} - \mu_{1,2})f_{1,2}(x_1)x_2 - \alpha_2 p_2 - D_2 p_2 . \quad (5e)$$

Notice that the incorporation of the time-scale effects, modelled in the same way as in the previous paper (Kooi *et al.*, 1998), differs from that done in (Rinaldi and Muratori,

1992a; Rinaldi and Muratori, 1992b; Muratori and Rinaldi, 1989; Muratori and Rinaldi, 1992). In those papers the maximum ingestion rate of the predator, $I_{1,2}$, is not multiplied by ε , only the maximum growth rate, $\mu_{1,2}$, is. As a result in their model the efficiency decreases when $\varepsilon \rightarrow 0$. Here, the maximum ingestion rate of the predator $I_{1,2}$ as well as its maximum growth rate $\mu_{1,2}$ are multiplied by ε . In this way the efficiency (ecology) or yield (microbiology) remains unchanged when ε is varied.

3 Model analysis

3.1 Parameter values

The full model (5) will be analysed using numerical bifurcation analysis. The parameter values are after (Nisbet *et al.*, 1983a) and given in Table 2. They are realistic for a two-trophic microbial food chain consisting of substrate, bacterium and ciliate. The values for the new parameters, the faeces recycle rates α_i are assumed to be the same as the maximum growth rate of the bacterium. The results are presented in one-parameter and two-parameter bifurcation diagrams. In a one-parameter bifurcation diagram the equilibrium biomass or extreme values during a limit cycle, are plotted as function of one bifurcation parameter for instance the nutrient input, whereby all other parameters are held constant. Parameter values at which the asymptotic dynamic behaviour changes suddenly, fix bifurcation points.

In some realistic cases, like a food chain of sewage-bacterium-worm (for example the water nymph *Nais elinguis*, a oligochaete species) often found in waste-water treatment plants (Ratsak *et al.*, 1993), there are differences in the order of magnitudes of the ingestion and growth rates. Parameter values for this model are also given in Table 2 and will be used when we do simulations associated with the aggregation technique.

3.2 Bifurcation analysis

For an introduction to bifurcation analysis the reader is referred to (Guckenheimer and Holmes, 1985; Kuznetsov, 1998) and to (Bazykin, 1998) for the application to ecosystem models. Bifurcation analysis gives information about the long-term dynamic behaviour of nonlinear dynamic systems. The structural stability is studied with respect to so-called free or bifurcation parameters. When such a parameter is varied, a value at which the asymptotic dynamics changes abruptly (for instance the solution becomes a stable limit cycle instead of a stable equilibrium) is called a bifurcation point. Numerical bifurcation packages, such as AUTO: (Doedel *et al.*, 1997) and LOCBIF, CONTENT: (Khibnik *et al.*, 1993; Kuznetsov and Levitin, 1997; Kuznetsov, 1998) are available to calculate bifurcation points.

Two bifurcations types appear to be important with the study of our model: the transcritical bifurcation which determines the boundary of coexistence of species in the parameter space and the Hopf bifurcation at which point the equilibrium of the system

becomes unstable and the asymptotic dynamics becomes oscillatory. The phenomenon that the system becomes unstable at higher levels of nutrient supply was found by Rosenzweig (Rosenzweig, 1971) with the Rosenzweig-MacArthur model for a predator–prey system and is known as the paradox of enrichment. Thereafter it was found analysing many related predator–prey models under various environmental conditions. Generally, the system not only starts to oscillate, but these oscillations become also severe.

A wide class of predator–prey models possess similar bifurcation diagrams, see for instance (Nisbet *et al.*, 1983b; Gurney and Nisbet, 1998). In these bifurcation diagrams the long-term dynamics is studied depending on environmental conditions. For the batch reactor the nutrient availability at the start of the experiment and the removal rate (due to harvesting or mortality) of the predator are often used as bifurcation parameters. In the chemostat case the natural bifurcation parameters are the concentration of the nutrients in the inflow and the dilution rate.

3.3 Perturbation theory

The reader is referred to (Hoppensteadt, 1993; Jones, 1995; Kevorkian and Cole, 1995) for an introduction to perturbation theory and to (Auger *et al.*, 2000a) for the application in ecological modelling. Regular perturbation theory deals with systems of the following form

$$\frac{dx}{d\tau} = f(x, y, \varepsilon), \quad (6a)$$

$$\frac{dy}{d\tau} = \varepsilon g(x, y), \quad (6b)$$

where $\varepsilon \in \mathbb{R}_+$ is small. Singular perturbation theory on the other hand deals with systems of the form:

$$\varepsilon \frac{dx}{dt} = f(x, y, \varepsilon), \quad (7a)$$

$$\varepsilon \frac{dy}{dt} = \varepsilon g(x, y), \quad (7b)$$

where $t = \varepsilon\tau$. Hence, τ is the fast time variable and t the slow variable. The terms regular and singular are used because the solutions depend regularly or singularly on ε at $\varepsilon = 0$ (Hoppensteadt, 1993). Notice that in the singular perturbation problem, when ε is put equal to zero in (7) these equations have a structural different form than the unperturbed original system.

With both cases, the first step consists in setting $\varepsilon = 0$ which gives the set of fast equilibria. In the first case, system (6), we get the fast system $d\bar{x}/d\tau = f(\bar{x}, y(0), 0)$. The equilibria of this differential equation are given by: $f(x, y, 0) = 0$. For small ε values the procedure consists in a limited expansion with respect to this parameter

$$\frac{dx}{d\tau} = f(x, y, 0) + \varepsilon \frac{\partial f}{\partial \varepsilon}(x, y, 0) + \dots \quad (8)$$

Thereafter (6b) is solved where the solution of the fast system \bar{x} is substituted.

In the second case, system (7), we get the algebraic equation of the so called “slow manifold”: $f(\bar{x}, \bar{y}, 0) = 0$. With good hypothesis, this is equivalent to $\bar{x} = F(\bar{y})$ and we can then substitute \bar{x} by $F(\bar{y})$ in the second equation, then: $d\bar{y}/dt = g(F(\bar{y}), \bar{y})$. Observe that we divided by ε as we are dealing with a singular perturbation problem. The procedure is generally mathematically justified by the application of a set of Theorems due to Fenichel (Fenichel, 1971; Jones, 1995).

Thus the main steps are:

1. Find the equilibria for the fast system (with $\varepsilon = 0$) defined by the time-derivatives of x_1 , p_1 and p_2 where x_2 serves as constant parameter.
2. Analyse the hyperbolic stability of these equilibria.
3. Substitute the stable equilibrium values in the derivatives of x_2 . This defines the slow system. When the fast equilibrium is stable, the slow system provides an approximation of the full system.

In some cases, there are multiple equilibria for the fast system, some are stable, the other are unstable. Here, we will deal with the case where there are two equilibria for which the stability condition depends on the value of the slow variables. After the fast transient, because of the dynamics of the slow variables, the stability of the two fast equilibria switches. In other words, there are two slow manifolds and the dynamics starts at one and suddenly it moves fast to the other one and continues there, leading to the stable equilibrium (Auger *et al.*, 2000b) or following a slow manifolds when it becomes unstable jumps suddenly to the first slow manifold again, and so on leading to a quasi-limit cycle (Kooi *et al.*, 1998).

4 Batch reactor conditions

The model under batch conditions, that is a closed system with no material exchange with the environment, is obtained from model (5) with $D_i = 0$, $i = 0, 1, 2$. The total biomass, for instance measured in C-mol, denoted by C and defined by

$$C(t) = x_0(t) + x_1(t) + p_1(t) + x_2(t) + p_2(t) , \quad (9)$$

is time-invariant, $C(t) = C(0)$, due to mass conservation. This equality will be used to eliminate the variable x_0 . By replacing x_0 by $C - x_1 - p_1 - x_2 - p_2$, system (5) with $D_i = 0$,

$i = 0, 1, 2$, reads:

$$\frac{dx_1}{d\tau} = x_1 \left(\mu_{0,1} \frac{C - x_1 - p_1 - x_2 - p_2}{k_{0,1} + C - x_1 - p_1 - x_2 - p_2} - m_1 \right) - \varepsilon I_{1,2} \frac{x_1 x_2}{k_{1,2} + x_1}, \quad (10a)$$

$$\frac{dx_2}{d\tau} = \varepsilon x_2 \left(\mu_{1,2} \frac{x_1}{k_{1,2} + x_1} - m_2 \right), \quad (10b)$$

$$\frac{dp_1}{d\tau} = (I_{0,1} - \mu_{0,1}) \frac{C - x_1 - p_1 - x_2 - p_2}{k_{0,1} + C - x_1 - p_1 - x_2 - p_2} x_1 - \alpha_1 p_1, \quad (10c)$$

$$\frac{dp_2}{d\tau} = \varepsilon (I_{1,2} - \mu_{1,2}) \frac{x_1}{k_{1,2} + x_1} x_2 - \alpha_2 p_2. \quad (10d)$$

This makes it possible to deal with the four dimensional full system for the state variables x_1, x_2, p_1, p_2 , where C is used as a bifurcation parameter.

The equilibria are with $\varepsilon = 1$

$$x_1^* = \frac{k_{1,2} m_2}{\mu_{1,2} - m_2}, \quad (11a)$$

$$x_2^* = \frac{k_{1,2} + x_1^*}{I_{1,2}} \left(\mu_{0,1} \frac{C - x_1^* - p_1^* - x_2^* - p_2^*}{k_{0,1} + C - x_1^* - p_1^* - x_2^* - p_2^*} - m_1 \right), \quad (11b)$$

$$p_1^* = \frac{(I_{0,1} - \mu_{0,1}) m_1}{\mu_{0,1} \alpha_1} x_1^*, \quad (11c)$$

$$p_2^* = \frac{(I_{1,2} - \mu_{1,2}) m_2}{\mu_{1,2} \alpha_2} x_2^*, \quad (11d)$$

where x_2^* is still given implicitly where the positive root of the resulting quadratic equation is taken.

The total biomass C has to be sufficient high to get coexistence of prey or even both prey and predator in the reactor. The value of C at the boundary of the region with coexistence, is called a transcritical bifurcation TC , one where only the prey can persist and one where the predator can persist too.

Mathematically the first point is found when the following conditions are satisfied. The equilibrium with biomass of the prey is zero, $\hat{x}_1 = \hat{x}_2 = 0$, is such that the growth rate of the prey is zero too, $dx_1/d\tau = 0$. That is, we are at the boundary of the region where the prey can invade the nutrient system. Equations (10c) and (10d) give $\hat{p}_1 = \hat{p}_2 = 0$. The resulting equations are

$$\hat{C} = \hat{x}_0, \quad (12a)$$

$$0 = \mu_{0,1} f_{0,1}(\hat{x}_0) - m_1. \quad (12b)$$

These two equations for the positive equilibrium values \hat{x}_0 fix the value \hat{C} . We obtain

$$\hat{C} = \hat{x}_0 = \frac{k_{0,1} m_1}{\mu_{0,1} - m_1}. \quad (13)$$

At the second transcritical bifurcation that marks the point where the predator can invade the nutrient–prey system, the equilibrium with biomass of the predator is zero, $\tilde{x}_2 = 0$ and furthermore the growth rate of the predator is zero too, $dx_2/d\tau = 0$. Equation (10d) gives directly $\tilde{p}_2 = 0$. The resulting equations are

$$\tilde{C} = \tilde{x}_0 + \tilde{x}_1 + \tilde{p}_1 , \quad (14a)$$

$$0 = \mu_{0,1}f_{0,1}(\tilde{x}_0) - m_1 , \quad (14b)$$

$$0 = \mu_{1,2}f_{1,2}(\tilde{x}_1) - m_2 , \quad (14c)$$

$$0 = (I_{0,1} - \mu_{0,1})f_{0,1}(\tilde{x}_0)\tilde{x}_1 - \alpha_1\tilde{p}_1 . \quad (14d)$$

Equations (14) give

$$\tilde{x}_0 = \frac{k_{0,1}m_1}{\mu_{0,1} - m_1} , \quad (15a)$$

$$\tilde{x}_1 = \frac{k_{1,2}m_2}{\mu_{1,2} - m_2} , \quad (15b)$$

$$\tilde{p}_1 = \frac{(I_{0,1} - \mu_{0,1})m_1\tilde{x}_1}{\mu_{0,1}\alpha_1} . \quad (15c)$$

Equation (14a) is a consequence of complete recycling of the nutrients which gives conservation, in this case in absence of the predator. Substitution of (15) in (14a) gives the transcritical bifurcation value \tilde{C} .

When increasing C , system (10) shows a Hopf bifurcation which marks the origin of oscillatory behaviour. No closed form expressions are available and we have to calculate this point numerically.

5 Two time scales batch reactor case

In this section, we study the case where two different time scales, that is small ε . The fast system is obtained by putting $\varepsilon = 0$ in system (10). It is formed by (10a), (10c and (10d) where \bar{x}_2 is treated as a parameter.

$$\frac{d\bar{x}_1}{d\tau} = \bar{x}_1 \left(\mu_{0,1} \frac{C - \bar{x}_1 - \bar{p}_1 - \bar{x}_2 - \bar{p}_2}{k_{0,1} + C - \bar{x}_1 - \bar{p}_1 - \bar{x}_2 - \bar{p}_2} - m_1 \right) , \quad (16a)$$

$$\frac{d\bar{p}_1}{d\tau} = (I_{0,1} - \mu_{0,1}) \frac{C - \bar{x}_2 - \bar{p}_2 - \bar{x}_1 - \bar{p}_1}{k_{0,1} + C - \bar{x}_2 - \bar{p}_2 - \bar{x}_1 - \bar{p}_1} \bar{x}_1 - \alpha_1 \bar{p}_1 , \quad (16b)$$

$$\frac{d\bar{p}_2}{d\tau} = -\alpha_2 \bar{p}_2 . \quad (16c)$$

The equilibria of this three-dimensional system for the three fast variables \bar{x}_1 , \bar{p}_1 and

\bar{p}_2 read

$$\bar{x}_1^* = \frac{\mu_{0,1}\alpha_1(C - \bar{x}_2 - \widehat{C})}{m_1(I_{0,1} - \mu_{0,1}) + \mu_{0,1}\alpha_1}, \quad (17a)$$

$$\bar{p}_1^* = \frac{(I_{0,1} - \mu_{0,1})m_1}{\mu_{0,1}\alpha_1} \bar{x}_1^*, \quad (17b)$$

$$\bar{p}_2^* = 0, \quad (17c)$$

where \bar{x}_2 is the slow variable of which the dynamics is described by an ordinary differential equation (ODE) derived below.

Because the ODE (16c) for \bar{p}_2 is decoupled from the two ODEs (16a) and (16b), it is sufficient to study their 2×2 Jacobian matrix evaluated at the equilibrium \bar{x}_1 and \bar{p}_1 given in (17a) and (17b). It can be shown that

- i) If $C < \widehat{C} + \bar{x}_2$ the equilibrium $(\bar{x}_1; \bar{p}_1; \bar{p}_2) = (0; 0; 0)$ is stable and is the unique non-negative equilibrium.
- ii) If $\widehat{C} + \bar{x}_2 < C$ the trivial equilibrium $(\bar{x}_1; \bar{p}_1; \bar{p}_2) = (0; 0; 0)$ is unstable and the non-trivial $(\bar{x}_1; \bar{p}_1; \bar{p}_2) = (\bar{x}_1^*; \bar{p}_1^*; 0)$ is stable and is the unique positive equilibrium.

These equilibria (17a) for x_1 , (17b) for p_1 and (17c) for p_2 , where \bar{x}_2 is a parameter, is substituted in (10b) with $\varepsilon = 0$. This yields the slow system for the slow variable \bar{x}_2

$$\frac{d\bar{x}_2}{dt} = \bar{x}_2 \left(\mu_{1,2} \frac{\bar{x}_1}{k_{1,2} + \bar{x}_1} - m_2 \right), \quad (18)$$

where $t = \varepsilon\tau$ again. The equilibrium is

$$\bar{x}_2^* = C - \frac{m_1 k_{0,1}}{\mu_{0,1} - m_1} - \frac{m_1(I_{0,1} - \mu_{0,1}) + \mu_{0,1}\alpha_1}{\mu_{0,1}\alpha_1} \frac{m_2 k_{1,2}}{\mu_{1,2} - m_2} = C - \widetilde{C}, \quad (19)$$

where we used (15). We conclude that

- i) If $C < \widehat{C}$ then $(\bar{x}_1; \bar{x}_2; \bar{p}_1; \bar{p}_2)$ approaches $(0; 0; 0; 0)$.
- ii) If $\widehat{C} < C < \widetilde{C}$ then $(\bar{x}_1; \bar{x}_2; \bar{p}_1; \bar{p}_2)$ approaches $(\bar{x}_1^*; 0; \bar{p}_1^*; 0)$. The slow system is

$$\frac{d\bar{x}_2}{dt} = -m_2 \bar{x}_2. \quad (20)$$

- iii) If $\widetilde{C} < C$ then $(\bar{x}_1; \bar{x}_2; \bar{p}_1; \bar{p}_2)$ approaches $(\bar{x}_1^*; \bar{x}_2^*; \bar{p}_1^*; 0)$. The resulting slow system is (18).

The points at which the reduced model changes, fixed by $C = \widehat{C}$ and $C = \widetilde{C}$ are transcritical bifurcation points for both the reduced model and the full model given in (14) and (15). With respect to this, the reduced model reflects the asymptotic dynamics of the full model well.

In Figures 2 and 3 simulation results for the prey and predator biomass densities, $x_1(\tau)$, $x_2(\tau)$, and for the nutrient density, $x_0(\tau)$, are depicted for the reduced and full model where $C = 300 > \tilde{C}$. After the transient, the solution of the reduced model is close to that of the full model. The differences for the equilibria of both models is explained as follows. Comparing (10b) and (18) gives that in equilibrium we have $\bar{x}_1^* = x_1^*$ and subsequently $\bar{p}_1^* = p_1^*$, see (10c) and (17b). The difference between \bar{x}_2^* and x_2^* is due to the fact that the consumption term of the predator feeding on the prey, $(\varepsilon I_{1,2} x_1 / (k_{1,2} + x_1)) x_2$ is neglected in (16a) and not in (10a). After $\tau \approx 600$, the biomass density of the predator $x_2(\tau)$ is large and this explains the difference between \bar{x}_2^* and x_2^* , and partly the difference between \bar{p}_2^* (17c) and p_2^* (11d). Furthermore we have $\bar{x}_0^* = \hat{C}$ and therefore \bar{x}_0^* is time-invariant. This follows directly from substitution of the expressions (17) in the expression for C in (9). This explains the difference between \bar{x}_0^* and x_0^* in Figure 3.

When $\varepsilon > 0$ there is a C so that the full system has a Hopf bifurcation. In Figure 4 we depict the two-parameter bifurcation diagram where C and ε are the bifurcation parameters. The curve denoted by H is the Hopf bifurcation curve that approaches the $\varepsilon = 0$ axis when $C \rightarrow \infty$. Hence, for a fixed strictly positive value of ε and when C is greater than its value on the H -curve (1200 in Figure 4), the reduced system has a stable equilibrium, as is shown in this section, while the full system converges to a stable limit cycle when time goes to infinity. In other words, the approximation is valid for a very small ε when C is large.

This illustrates that for practical cases when $\varepsilon > 0$, the reduced system gives not always good approximations for the long-term dynamics. In the next section we deal with the chemostat case where we retain first-order terms with the construction of an reduced model. This gives a better long-term approximation. Such an approach can be applied with batch conditions discussed here in the same manner.

6 Chemostat conditions

The model under chemostat conditions, is obtained from model (5) with $D_i = D$, $i = 0, 1, 2$. We define now the total biomass measured in C-mol $H(t)$ by

$$H(t) = x_0(t) + x_1(t) + x_2(t) + p_1(t) + p_2(t) . \quad (21)$$

By replacing x_0 by $H - x_1 - p_1 - x_2 - p_2$, system (5) with $D_i = D$, $i = 0, 1, 2$, reads:

$$\frac{dH}{d\tau} = -\varepsilon D(H - x_r) , \quad (22a)$$

$$\frac{dx_1}{d\tau} = x_1 \left(\mu_{0,1} \frac{H - x_1 - p_1 - x_2 - p_2}{k_{0,1} + H - x_1 - p_1 - x_2 - p_2} - m_1 - \varepsilon D - \varepsilon I_{1,2} \frac{x_2}{k_{1,2} + x_1} \right) , \quad (22b)$$

$$\frac{dx_2}{d\tau} = \varepsilon x_2 \left(\mu_{1,2} \frac{x_1}{k_{1,2} + x_1} - m_2 - D \right) , \quad (22c)$$

$$\frac{dp_1}{d\tau} = (I_{0,1} - \mu_{0,1}) \frac{H - x_2 - p_2 - x_1 - p_1}{k_{0,1} + H - x_2 - p_2 - x_1 - p_1} x_1 - \alpha_1 p_1 - \varepsilon D p_1 , \quad (22d)$$

$$\frac{dp_2}{d\tau} = \varepsilon (I_{1,2} - \mu_{1,2}) \frac{x_1}{k_{1,2} + x_1} x_2 - \alpha_2 p_2 - \varepsilon D p_2 . \quad (22e)$$

First we analyse this model where $\varepsilon = 1$ with numerical bifurcation techniques. The two-parameter bifurcation diagram for the model with and without nutrient recycling is given in Figure 5. The transcritical bifurcation curve which determines the boundary of coexistence of species in the parameter space is denoted by TC_r and the Hopf bifurcation curve, that bounds the region where the system oscillates, is denoted by H_r . We recall that the parameter values given in Table 2 are from (Nisbet *et al.*, 1983a). The transcritical bifurcation curve TC and Hopf bifurcation curve H are the two bifurcation curves for that model without nutrient recycling, thus $\alpha_1 = \alpha_2 = 0$.

For a fixed dilution rate the density of the nutrient in the inflow has to be sufficiently high to get coexistence of both prey and predator in the reactor. Equations similar to those for the batch reactor (14), describe this transcritical bifurcation. The following substitutions have to be made: $C \rightarrow H$ and $m_i \rightarrow m_i + D$ and $\alpha_1 \rightarrow \alpha_1 + D$. In this way we obtain now a relationship between the two parameters D and x_r , that is, the function $\tilde{x}_r(D)$ of which the graph is the bifurcation curve TC_r in Figure 5.

When the nutrient supply is increased further, the positive equilibrium becomes unstable at a Hopf bifurcation H and a stable limit cycle originates. At that point the real part of two complex conjugate eigenvalues equals zero. Explicit expressions for the relationship between the two parameters D and x_r do not exist. Therefore, the Hopf bifurcation curve has to be approximated numerically.

In Figure 6 the long-term biomass values for the predator x_2 are depicted as a function of x_r for a fixed $D = 0.08$. If x_r is lower than its transcritical bifurcation TC_r value the prey is the only organism in the reactor. If the x_r -value is higher than its TC_r -value the predator can invade the system when it is introduced in small amounts and there is a stable coexistence. When x_r is increased and the H_r -value is reached, this equilibrium becomes unstable. For higher x_r values the system oscillates and the maximum and minimum values of the stable limit cycles are plotted in Figure 6. With rather high x_r values the minimum values become very low. For comparison in Figure 6 results are also given for the nutrient-prey-predator model without recycling, $\alpha_1 = \alpha_2 = 0$, also for $D = 0.08$.

7 Two time scales chemostat reactor case

We will now apply the singular perturbation theory in the case that the prey dynamics feeding on nutrient is fast and that the predator dynamics feeding on the prey is slow ($\varepsilon \ll 1$) is formed by the two ODEs (22b) and (22d). We will consider a zero-order approximation and a first-order approximation where all ε terms are retained. The bifurcation analysis of the resulting fast system can be done analytically for the zero-order approximation. For the first-order approximation we have to resort to calculated bifurcation diagrams.

7.1 Zero-order approximations

The fast system is exactly the same as in the batch reactor case (16) where constant C has to be replaced by \bar{H} which is now an extra parameter, and we introduce $\hat{H} = \hat{C} = m_1 k_{0,1} / (\mu_{0,1} - m_1)$.

The two dimensional slow system for the variables \bar{H} and \bar{x}_2 reads

$$\frac{d\bar{H}}{dt} = -D(\bar{H} - x_r), \quad (23a)$$

$$\frac{d\bar{x}_2}{dt} = \bar{x}_2 \left(\mu_{1,2} \frac{\bar{x}_1}{k_{1,2} + \bar{x}_1} - m_2 - D \right), \quad (23b)$$

where for \bar{x}_1 the expression (17a) is substituted. Similar to the batch case we introduce

$$\tilde{H} = \frac{m_1 k_{0,1}}{\mu_{0,1} - m_1} + \frac{m_1 (I_{0,1} - \mu_{0,1}) + \mu_{0,1} \alpha_1 (m_2 + D) k_{1,2}}{\mu_{0,1} \alpha_1 (\mu_{1,2} - m_2 - D)}. \quad (24)$$

Then, the equilibria are

$$\bar{H}^* = x_r, \quad (25)$$

$$\bar{x}_2^* = x_r - \tilde{H}. \quad (26)$$

We conclude that

- i) If $x_r < \hat{H}$ then $(x_1; x_2; p_1; p_2)$ approaches $(0; 0; 0; 0)$,
- ii) If $\hat{H} < x_r < \tilde{H}$ then $(x_1; x_2; p_1; p_2)$ approaches $(x_1^*; 0; p_1^*; 0)$,
- iii) If $\tilde{H} < x_r$ then $(x_1; x_2; p_1; p_2)$ approaches $(x_1^*; x_2^*; p_1^*; 0)$.

Notice that contrary to the batch reactor case, the slow system is now two-dimensional instead of one. In the batch reactor case C serves as a constant while here H is a variable which converges to a constant x_r for time goes to infinity. This mathematical detail has large consequences. The bifurcation diagram Figure 5 shows that for $D > 0$ the full system becomes unstable when x_r is increased and the Hopf bifurcation curve H_r is passed, while the reduced system where $D = 0$ is assumed in deriving the fast system, has still a stable equilibrium in those situations. Hence the zero-order approximation approach fails when this occurs. Therefore we propose a first-order approximation in the next subsection.

7.2 First-order approximation

The terms proportional to $\varepsilon I_{1,2}$ as well as εD are retained and this yields the first-order approximation. The fast system reduces to the three ODEs, (22b), (22d) and (22e).

The two slow variables \bar{H} and \bar{x}_2 are now parameters of the fast system. For small values of x_r there is a stable interior equilibrium. However, when x_r is large the full system has multiple equilibria as a consequence of the predator consumption term proportional to $\varepsilon I_{1,2}$, and this complicates the analysis and therefore we perform a numerical bifurcation analysis where we used LOCBIF. In (Kooi *et al.*, 1998) we derived analytic expressions for the chemostat case without recycling and maintenance: $\alpha_i = m_i = 0$, $i = 1, 2$.

The calculated bifurcation one-parameter diagram is shown in Figure 7 where $x_r = 1600$ and $D = 0.001$. The single bifurcation parameter is the slow variable \bar{x}_2 . When asymptotic dynamics is concerned, it is sufficient to consider $H(t) = x_r$, (Thieme, 1992; Smith and Waltman, 1994) and since we are mainly interested the long-term dynamics, we took $\bar{H}(t) = x_r$. There are two stable slow manifolds, AD and BC , and one unstable slow manifold, AC . The multiple solutions are the trivial solution $\bar{x}_2 = 0$ and two roots of a quadratic equation obtained by taking the right-hand side of (22b) equal zero. Observe that the fact that the resulting equation is quadratic in \bar{x}_1 results from the predator consumption term proportional to $\varepsilon I_{1,2}$ which was neglected in the zero-order approximation. A transcritical bifurcation, where the graph of the quadratic function crosses the \bar{x}_1 axis, is denoted by \bar{x}_{2TC} and a tangent bifurcation, where the discriminant of this quadratic function is zero, is denoted by \bar{x}_{2T} .

Depending on the initial conditions $\bar{x}_1(0)$, $\bar{p}_1(0)$ and $\bar{p}_2(0)$, as well as $\bar{x}_2(0)$, the system converges quickly towards a stable equilibrium of the fast system. When $\bar{x}_2(0) < \bar{x}_{2TC}$ it goes to the positive stable part of the non-trivial branch (left side of D) and when $\bar{x}_2(0) > \bar{x}_{2TC}$ to the stable part of the trivial branch (right side of B).

When $\bar{x}_{2TC} < \bar{x}_2(0) < \bar{x}_{2T}$ there are two stable equilibria of the fast system. If $\bar{x}_1(0)$ lies below the curve AC in Figure 7, the system converges quickly to the trivial branch (between B and C). If on the other hand $\bar{x}_1(0)$ lies above the curve AC, the system goes to the non-trivial branch (between A and D). In other words, the unstable fast manifold, curve AC is a separatrix.

When the two parameters x_r and D are so that $\bar{x}_{1T} < x_1^* = (m_2 + D)k_{1,2}/(\mu_{1,2} - m_2 - D)$ there is a stable equilibrium and both reduced and full system converge when time goes to infinity to this positive equilibrium. If, on the other hand, $\bar{x}_{1T} > x_1^*$ then the reduced system possesses a quasi-limit cycle, such as the trajectory ABCD in Figure 7, while the full system shows a limit cycle also shown in Figure 7. Hence, this figure is also the phase-plane plot for the full system where $x_r = 1600$ and $D = 0.001$.

Observe that generally when $H \neq x_r$ these manifolds move slowly. On the stable trivial fast equilibrium manifold BC the asymptotic dynamics is described by

$$\frac{d\bar{H}}{dt} = -D(\bar{H} - x_r) \quad (27a)$$

$$\frac{d\bar{x}_2}{dt} = -D\bar{x}_2, \quad (27b)$$

where $\bar{x}_1 = 0$ and $\bar{p}_1 = 0$ are substituted in (22a) and (22c). On the stable non-trivial fast equilibrium manifold DA the dynamics is described by (22a) and (22c)

$$\frac{d\bar{H}}{dt} = -D(\bar{H} - x_r) \quad (28a)$$

$$\frac{d\bar{x}_2}{dt} = \bar{x}_2 \left(\mu_{1,2} \frac{\bar{x}_1}{k_{1,2} + \bar{x}_1} - m_2 - D \right), \quad (28b)$$

where \bar{x}_1 and \bar{p}_1 are the solutions of the equilibrium equations (22b) and (22d).

Subsequently for both the trivial and non-trivial equilibrium manifolds the density of the nutrient, $\bar{x}_0(t)$, may be calculated by the conservation relationship: $\bar{x}_0(t) = x_r - \bar{x}_1(t) - \bar{p}_1(t) - \bar{x}_2(t) - \bar{p}_2(t)$. In Figure 7 we show these solutions for the reduced system $\bar{x}_1(t)$ and $\bar{x}_2(t)$ as well as the stable limit cycle of the full system $x_1(t)$ and $x_2(t)$.

8 Discussion and conclusions

In the batch reactor the system where recycling of the nutrient takes place, evolves to a state where the biomass is distributed over the different trophic levels, while without recycling all biomass ends finally at the predator level and the other levels are exhausted.

In (Nisbet *et al.*, 1983b) it is shown that with the Monod model being a special case of the Monod-Herbert model where $m_i = 0$, $i = 1, 2$, the transcritical bifurcation curve TC and the Hopf bifurcation curve H intersect the horizontal axis where $D = 0$. The results for the Monod-Herbert model depicted in Figure 5, and already given in (Nisbet *et al.*, 1983a), show that these bifurcation curves TC and H do not intersect the $D = 0$ axis but approach this axis when x_r goes to infinity. That is a stable equilibrium exists for non-zero, but possibly small, dilution rates. From these results it was concluded in (Nisbet *et al.*, 1983a) that maintenance has a stabilising effect. In Figure 5 the curves TC_r and H_r where maintenance is modelled and also nutrient recycling is taken into account the bifurcation curves intersect the $D = 0$ axis as with the Monod model. Thus, nutrient recycling counteracts the stabilising effect of maintenance.

In Figure 6 the biomasses are given for the model with and without recycling, that is the Monod-Herbert model. Comparing the results for both models shows that for model (22) the oscillations are more severe and at troughs in the cycle the biomasses can become very small. However, when this occurs, the deterministic model formulation fails to hold true and extinction due to demographic stochasticity is likely (Rosenzweig, 1971).

Figures 2 and 3 illustrate the power of the aggregation technique. After the short transient, the solution of the reduced model is close to that of the full model. The transcritical bifurcations of the reduced model and full model, which terminates invasion of the prey trophic level, occur at exactly the same bifurcation parameter values, \hat{C} and \tilde{C} .

For large C -values, however, the time scales have to differ a lot ($\varepsilon\mu_{1,2}/\mu_{0,1} \ll 1$) in order to obtain reasonable approximations. When ε is not small enough, the solution of the full model converges to a stable limit cycle while the solution of the reduced model

converges to a stable equilibrium. A first-order approximation approach would give the same qualitative long-term dynamics for both the full and the reduced model.

The zero-order approximation in the chemostat case, indicates a stable equilibrium for the reduced model (where $D = 0$) and a limit cycle for the full model (when $D > 0$ but small). Obviously a hypothesis for applicability of the Fenichel Theorem is not satisfied. This can be explained in biological terms as follows. With $D = 0$ the reservoir, from which the nutrient is supplied into the reactor, is decoupled from the chemostat reactor and the situation resembles the batch reactor case. Hence, the parameter x_r is meaningless when $D = 0$. As a result, as time goes to infinity the total biomass H converges to x_r if $D > 0$, but is time-invariant when $D = 0$. Since in the aggregation approach the dilution rate D is multiplied by the perturbation parameter ε , there is a discontinuity for $\varepsilon = 0$.

The first-order approximation approach gives a better long-term approximation without extra computational efforts. With the first-order approximation reduced model for the chemostat case, the transcritical bifurcations of the reduced model and full model occur at exactly the same bifurcation parameter values. Furthermore, the tangent bifurcation parameter values of the reduced model coincide with those at the Hopf bifurcation of the full system. This implies that the reduced and full model start to oscillate when x_r is increased leaving D unchanged, at exactly the same parameter value.

The differences between the quasi-limit cycle of the reduced system and the limit cycle of the full system shown in Figure 7 are related to the “delayed bifurcations” associated with the tangent and transcritical bifurcations of the reduced system, see (Diener and Diener, 1983; Eckhaus, 1983; Schecter, 1985; Rinaldi and Muratori, 1992b; De Feo and Rinaldi, 1998). This phenomenon is more significant when in the parameter space the system is close to a bifurcation point.

In this article we show that bifurcation theory and singular perturbation theory provide tools for the analyse of mathematical models of simple ecosystems when different time scales for the trophic levels exist. The reduced model is lower dimensional and is therefore easier to handle analytically and numerically. Numerical simulation of the reduced model requires less computing time important with sensitivity studies and parameter estimation. Application of the zero-order approximation perturbation technique does in the chemostat case not always yield useful results. We showed that in those cases a first-order approximation is needed to get the same qualitative long-term dynamics for both the full and the reduced model.

References

- Aota, Y. and Nakajima, H., 2000. Mathematical analysis on coexistence conditions of phytoplankton and bacteria systems with nutrient recycling. *Ecological Modelling*, 135: 17–31.
- Auger, P., Charles, S., Viala, M., and Poggiale, J. C., 2000a. Aggregation and emergence of ecological modelling: integration of ecological levels. *Ecological Modelling*, 127: 11–20.

- Auger, P. and Poggiale, J. C., 1996. Emergence of population growth models : Fast migration and slow growth. *Journal of Theoretical Biology*, 182: 99–108.
- Auger, P., Poggiale, J. C., and Charles, S., 2000b. Emergence of individual behaviour at the population level. Effects of density-dependent migration on population dynamics. *Comptes rendus de l'Academie des science series III-Sciences de la vie-life*, 323: 119–127.
- Bazykin, A. D., 1998. *Nonlinear dynamics of interacting populations*. Singapore: World Scientific, 216 pp.
- Beretta, E., Bischi, G. I., and Solimano, F., 1990. Stability in chemostat equations with delayed nutrient recycling. *Journal of Mathematical Biology*, 28: 99–111.
- De Feo, O. and Rinaldi, S., 1998. Singular homoclinic bifurcations in tri-trophic food chains. *Mathematical Biosciences*, 148: 7–20.
- DeAngelis, D. L., 1992. *Dynamics of Nutrient Cycling and Food Webs*. Number 9 in Population and Community Biology series. London: Chapman & Hall, 270 pp.
- Diener, F. and Diener, M., 1983. Seven formulas concerning canards. *Comptes rendus de l'Academie des science*, 297: 577–580.
- Doedel, E. J., Champneys, A. R., Fairgrieve, T. F., Kuznetsov, Y. A., Sandstede, B., and Wang, X., 1997. *AUTO 97: Continuation and Bifurcation software for ordinary differential equations*. Technical report, Concordia University, Montreal, Canada.
- Eckhaus, W., 1983. Relaxation oscillations including a standard chase on french ducks. In *Asymptotic analysis II*, volume 985 of *Lecture Notes in Mathematics* : 449–494. Berlin: Springer-Verlag.
- Fenichel, N., 1971. Persistence and smoothness of invariant manifolds for flows. *Indiana University Mathematical Journal*, 21: 193–226.
- Guckenheimer, J. and Holmes, P., 1985. *Nonlinear Oscillations, Dynamical Systems and Bifurcations of Vector Fields*, volume 42 of *Applied Mathematical Sciences*. New York: Springer-Verlag, 2 edition.
- Gurney, W. S. C. and Nisbet, R. M., 1998. *Ecological Dynamics*. Oxford University Press, 335 pp.
- Hoppensteadt, F. C., 1993. *Analysis and Simulation of Chaotic Systems*. Applied Mathematical Sciences. Berlin: Springer-Verlag.
- Iwasa, Y., Andreasen, V., and Levin, S. A., 1987. Aggregation in model ecosystems I. perfect aggregation. *Ecol. Modelling*, 37: 287–302.
- Iwasa, Y., Levin, S. A., and Andreasen, V., 1989. Aggregation in model ecosystems II. approximate aggregation. *IMA J. Math. Appl. Med. Biol.*, 6: 1–23.
- Jones, C. K. R. T., 1995. Geometric singular perturbation theory. *Dynamical Systems*, 1609: 44–118.

- Kevorkian, J. and Cole, J., 1995. *Multiple Scale and Singular Perturbation Methods*, volume 114 of *Applied Mathematical Sciences*. Berlin: Springer-Verlag.
- Khibnik, A. I., Kuznetsov, Y. A., Levitin, V. V., and Nikolaev, E. V., 1993. Continuation techniques and interactive software for bifurcation analysis of ODEs and iterated maps. *Physica D*, 62: 360–371.
- Kooi, B. W., Poggiale, J. C., and Auger, P., 1998. Aggregation methods in food chains. *Mathematical Computer Modelling*, 27: 109–120.
- Kooijman, S. A. L. M., 2000. *Dynamic Energy and Mass Budgets in Biological Systems*. Cambridge: Cambridge University Press.
- Kooijman, S. A. L. M. and Nisbet, R. M., 2000. How light and nutrients affect life in a closed bottle. In S. E. Jørgenson (Editor), *Thermodynamics and ecology* : 19–60.: CRC Publ.
- Kuznetsov, Y. A., 1998. *Elements of Applied Bifurcation Theory*, volume 112 of *Applied Mathematical Sciences*. New York: Springer-Verlag, 2 edition.
- Kuznetsov, Y. A. and Levitin, V. V., 1997. *CONTENT: Integrated environment for the analysis of dynamical systems*. Centrum voor Wiskunde en Informatica (CWI), Kruislaan 413, 1098 SJ Amsterdam, The Netherlands, 1.5 edition.
- Muratori, S. and Rinaldi, S., 1989. A dynamical system with hopf bifurcations and catastrophes. *Appl. Math. Comp.*, 29: 1–15.
- Muratori, S. and Rinaldi, S., 1992. Low- and high-frequency oscillations in three-dimensional food chain systems. *SIAM J. Appl. Math.*, 52: 1688–1706.
- Nisbet, R. M., Cunningham, A., and Gurney, W. S. C., 1983a. Endogenous metabolism and the stability of microbial prey-predator systems. *Biotechnol. Bioeng.*, 25: 301–306.
- Nisbet, R. M. and Gurney, W. S. C., 1976. Model of material cycling in a closed ecosystem. *Nature*, 264: 633–634.
- Nisbet, R. M., McKinstry, J., and Gurney, W. S. C., 1983b. A strategic model of material cycling in a closed ecosystem. *Mathematical Biosciences*, 64: 99–113.
- Poggiale, J. C. and Auger, P., 1996. Fast oscillating migrations in a predator-prey model. *Mathematical Models & Methods in Applied Sciences (M3AS)*, 6: 217–226.
- Ratsak, C. H., Kooijman, S. A. L. M., and Kooi, B. W., 1993. Modelling the growth of an oligocheate on activated sludge. *Wat. Res.*, 27: 739–747.
- Rinaldi, S. and Muratori, S., 1992a. Limit-cycles in slow fast forest pest models. *Theoretical Population Biology*, 41: 26–43.
- Rinaldi, S. and Muratori, S., 1992b. Slow fast limit-cycles in predator prey models. *Ecological Modelling*, 61: 287–308.
- Rosenzweig, M. L., 1971. Paradox of enrichment: destabilization of exploitation ecosystems in ecological time. *Science*, 171: 385–387.

- Ruan, S., 1993. Persistence and coexistence in zooplankton–phytoplankton–nutrient models with instantaneous nutrient recycling. *Journal of Mathematical Biology*, 31: 633–654.
- Ruan, S., 2001. Oscillations in plankton models nutrient recycling. *Journal of Theoretical Biology*, 208: 15–26.
- Schechter, S., 1985. Persistent unstable equilibria and closed orbits of a singularly perturbed equation. *J. Diff. Eqn.*, 60: 131–141.
- Smith, H. L. and Waltman, P., 1994. *The Theory of the Chemostat*. Cambridge: Cambridge University Press, 313 pp.
- Thieme, H., 1992. Convergence results and a Poincaré-Bendixon trichotomy for asymptotically autonomous differential equations. *Journal of Mathematical Biology*, 30: 755–763.

Table 1: Parameters and state variables for both full and reduced model: t=time, m=biomass, v=volume of the region of interest.

Parameter	Unit	Interpretation
t	t	Time
τ	t	Fast time variable
x_0	$\text{m} \cdot \text{v}^{-1}$	Nutrient density
x_i	$\text{m} \cdot \text{v}^{-1}$	Biomass density
x_r	$\text{m} \cdot \text{v}^{-1}$	Nutrient concentration in reservoir
D	t^{-1}	Dilution rate
m_i	t^{-1}	Maintenance rate coefficient
$k_{i-1,i}$	$\text{m} \cdot \text{v}^{-1}$	Saturation constant
$I_{i-1,i}$	t^{-1}	Food uptake rate coefficient
$\mu_{i-1,i}$	t^{-1}	Population growth rate coefficient
$y_{i-1,i}$	—	Yield
α_i	t^{-1}	Faeces recycle rate
β_i	t^{-1}	Metabolic products recycle rate

Table 2: Parameter set for the substrate-bacterium-ciliate model ($\varepsilon = 1$) after (Nisbet *et al.*, 1983a), and the substrate-bacterium-worm model ($\varepsilon \ll 1$) after (Kooi *et al.*, 1998). In both cases we have $I_{i-1,i} = \mu_{i-1,i}/y_{i-1,i}$ and $m_i = 0.05\mu_{i-1,i}$. The values for the faeces recycle rates α_i , $i = 1, 2$ are taken equal to the maximum growth rate of the prey $\mu_{0,1}$. The nutrient density and the biomass density as well as the saturation constants $k_{i-1,i}$ measured in gram can be converted in C-mol with 24.6 gram dry weight per C-mol (Kooijman, 2000), where we assume that the chemical composition of the nutrient, prey and predator are the same for the sake simplicity.

Parameter	Units	$i = 1$	$i = 2$	
			$\varepsilon = 1$	$\varepsilon \ll 1$
$y_{i-1,i}$	—	0.4	0.6	0.6
$\mu_{i-1,i}$	h^{-1}	0.5	0.2	0.01
$k_{i-1,i}$	mg dm^{-3}	8	9	50

Figure captions

Figure 1: Material fluxes through the food chain with recycling. Food is ingested with rate $I_{i-1,i}f_{i-1,i}x_i$. Per unit of time, the part $(I_{i-1,i} - \mu_{i-1,i})f_{i-1,i}x_i$ is unusable and transferred into faeces p_i . The faeces are decomposed at an exponential decay rate α_i . Maintenance-associated products z_i are formed at a rate m_ix_i . These products are decomposed at an exponential decay rate β_i .

Figure 2: The biomasses of the predator and prey for the full system x_2, x_1 and the reduced system \bar{x}_2, \bar{x}_1 as a function of time t , with $C = 300$ and initial conditions: $x_0(0) = 145$, $x_1(0) = 150$, $p_1(0) = 0$, $x_2(0) = \bar{x}_2(0) = 5$ and $p_2(0) = 0$. Solid lines are for the full system $x_i(t)$, and dashed lines are for the reduced system $\bar{x}_i(t)$, $i = 1, 2$.

Figure 3: The nutrient density for the full system x_0 and the reduced system \bar{x}_0 as a function of time t , with $C = 300$. Initial conditions as in Figure 2 thus $x_0(0) = 145$. Solid lines are for the full system $x_0(t)$ and dashed lines are for the reduced system $\bar{x}_0(t)$.

Figure 4: Two-parameter bifurcation diagram for the model under the batch conditions (10). The bifurcation parameters are ϵ and the initial biomass in the reactor C . Values assigned to physiological parameters and reference values for the perturbation parameters are listed in Table 2. The curve H marks supercritical Hopf bifurcation curves.

Figure 5: Two-parameter bifurcation diagram for the predator–prey model in the chemostat with ($\alpha_1 = \alpha_2 = 0.5$) and without ($\alpha_1 = \alpha_2 = 0$) recycling (22). The bifurcation parameters are the dilution rate D and the nutrient concentration in reservoir x_r . Values assigned to physiological parameters and reference values for the perturbation parameters are listed in Table 2. The curves TC, TC_r mark transcritical bifurcation curves, H and H_r mark supercritical Hopf bifurcation curves.

Figure 6: One-parameter bifurcation diagram for the predator–prey model in the chemostat with ($\alpha_1 = \alpha_2 = 0.5$) and without ($\alpha_1 = \alpha_2 = 0$) recycling (22). The bifurcation parameter is the nutrient concentration in reservoir x_r where $D = 0.08$. Values assigned to physiological parameters and reference values for the perturbation parameters are listed in Table 2. Solid curves are the stable equilibria and the extreme values of the stable limit cycles. Dashed curves indicate the unstable equilibria.

Figure 7: Phase-plane plot for the full system as well as the one-parameter bifurcation diagram of fast system of the model with recycling (22) where $x_r = 1600 \text{ mg dm}^{-3}$ and $D = 0.001 \text{ h}^{-1}$. Values assigned to physiological parameters and reference values for the perturbation parameters are listed in Table 2 for $\epsilon \ll 1$. The closed solid curve is the limit cycle $(x_1(t), x_2(t))$ for full system. The trajectory ABCD is the quasi-limit cycle for reduced system. Point A indicates a tangent bifurcation point and point C a transcritical bifurcation point, both for the reduced system. Two stable branches of the fast equilibrium manifolds are B→C and D→A. The fast unstable equilibrium manifold curve AC is the separatrix.

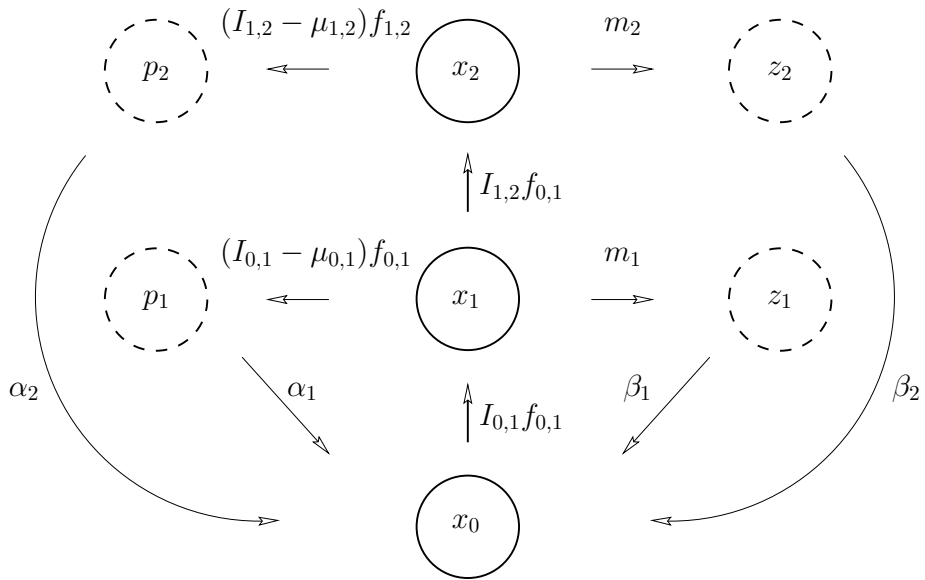


Figure 1:

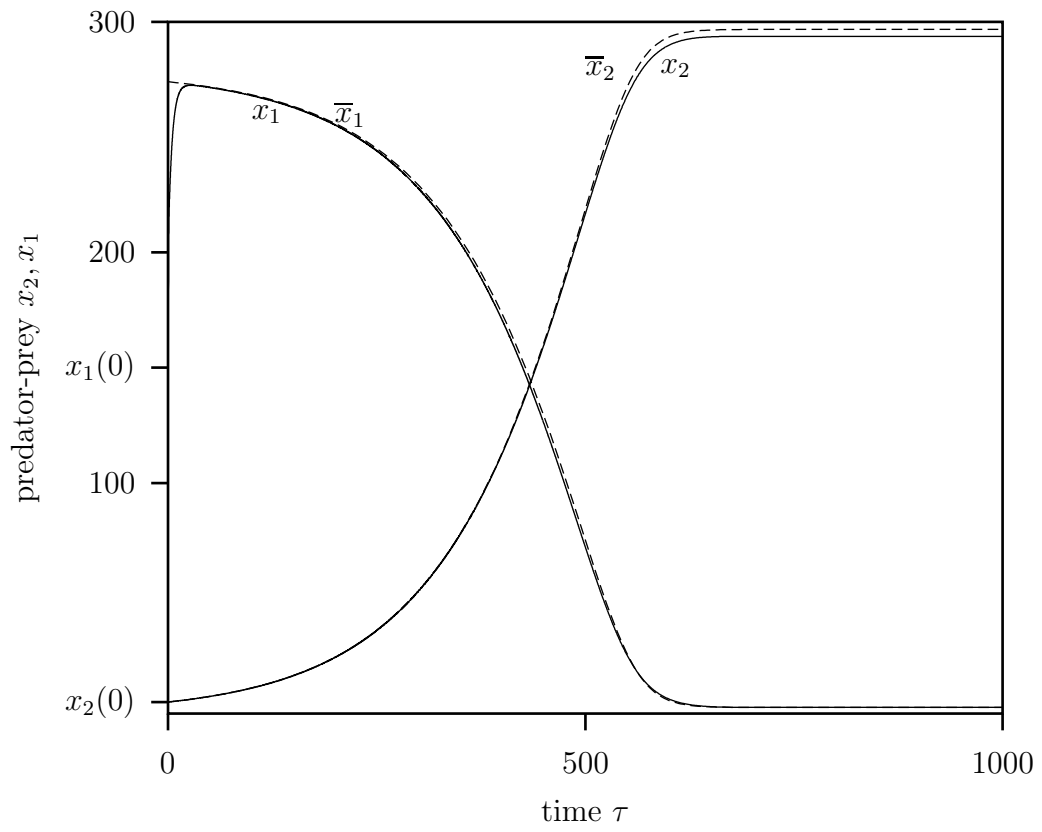


Figure 2:

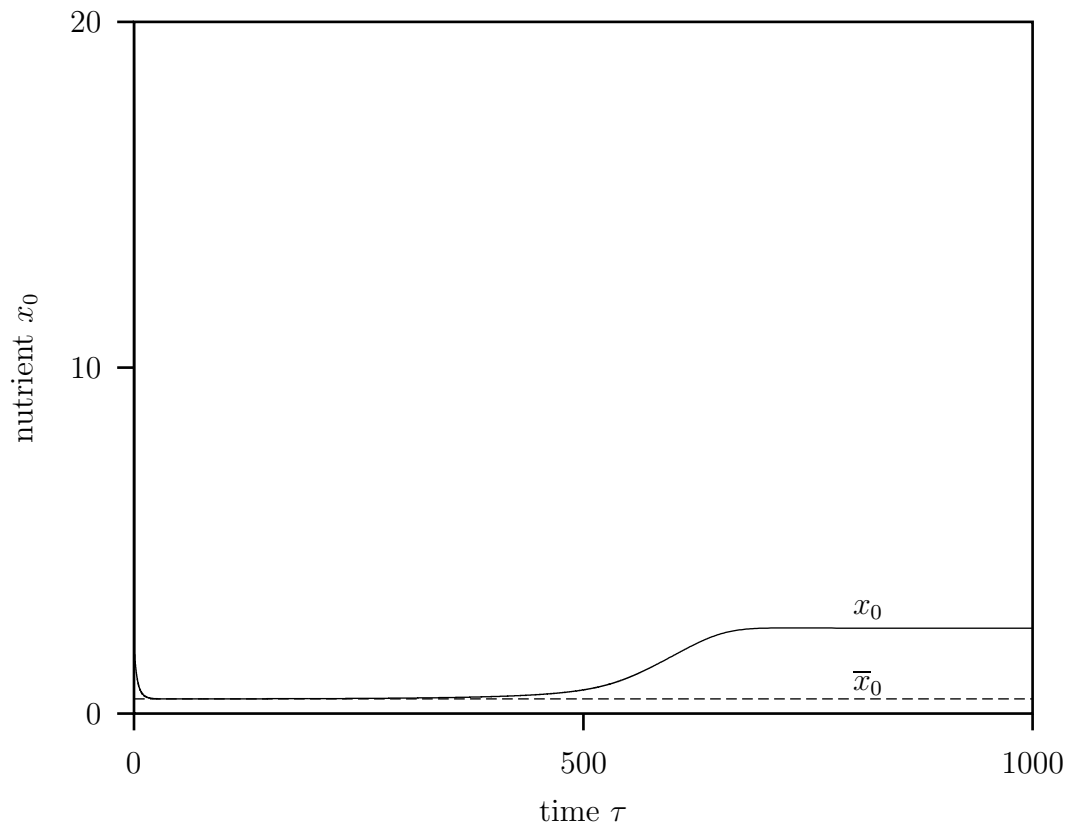


Figure 3:

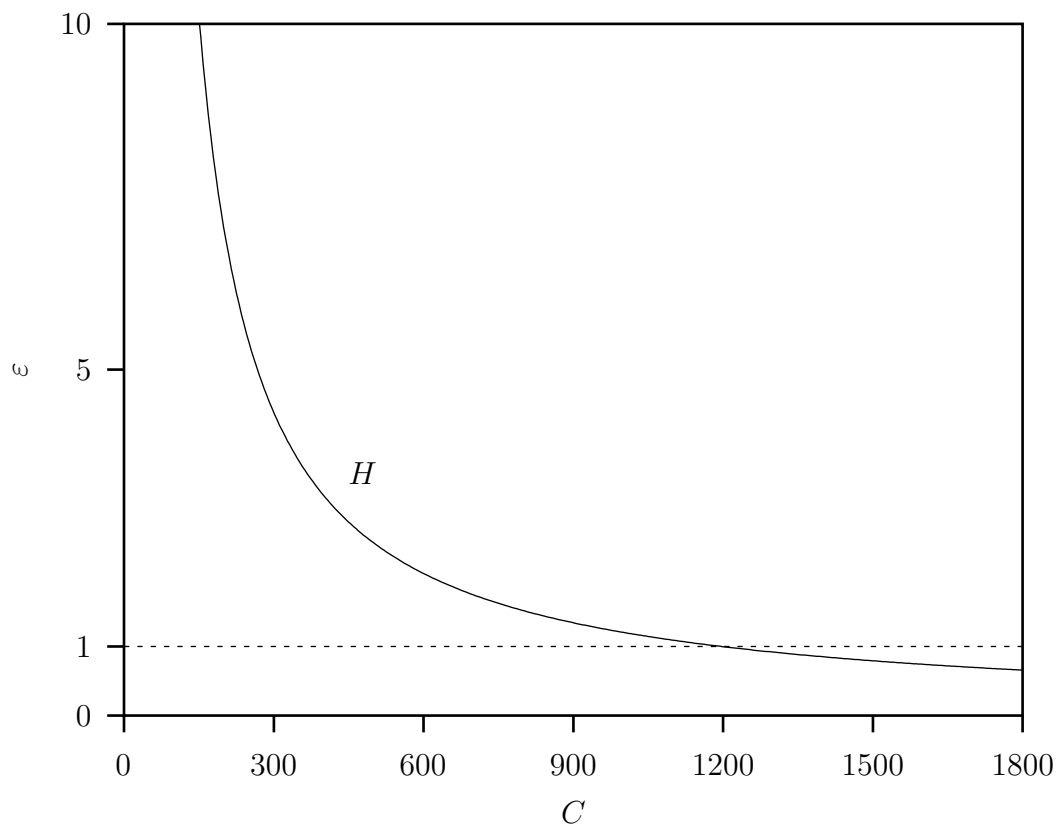


Figure 4:

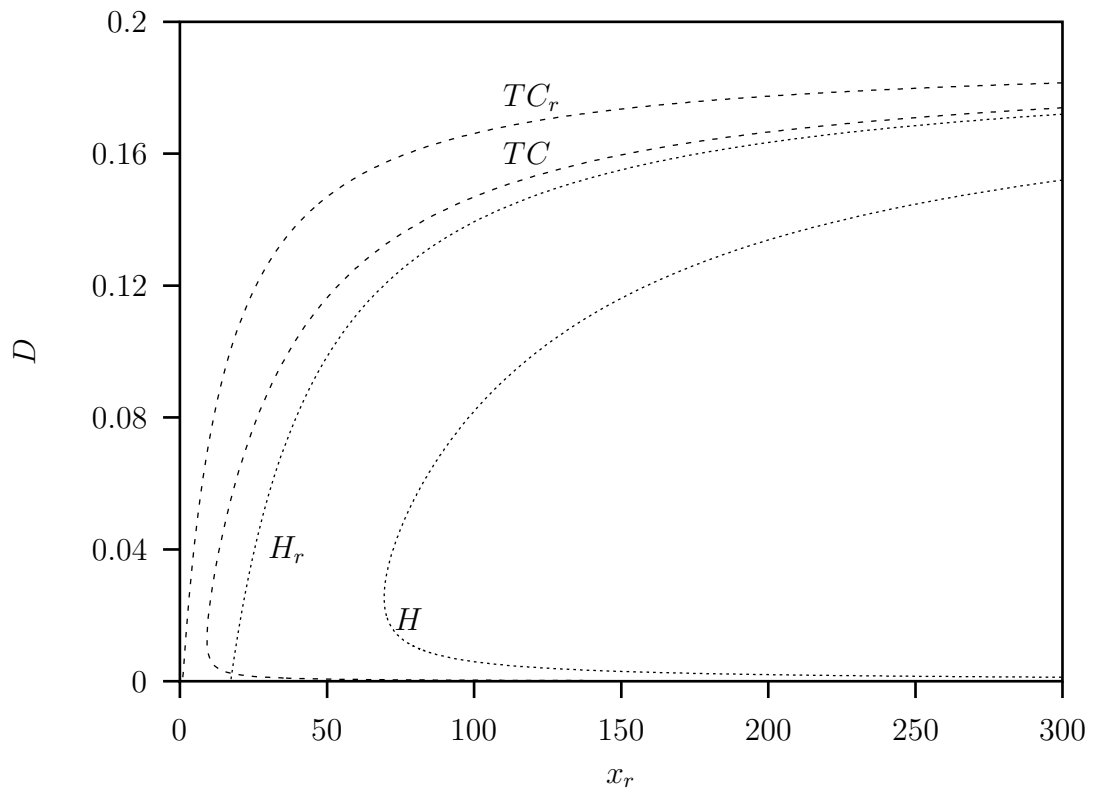


Figure 5:

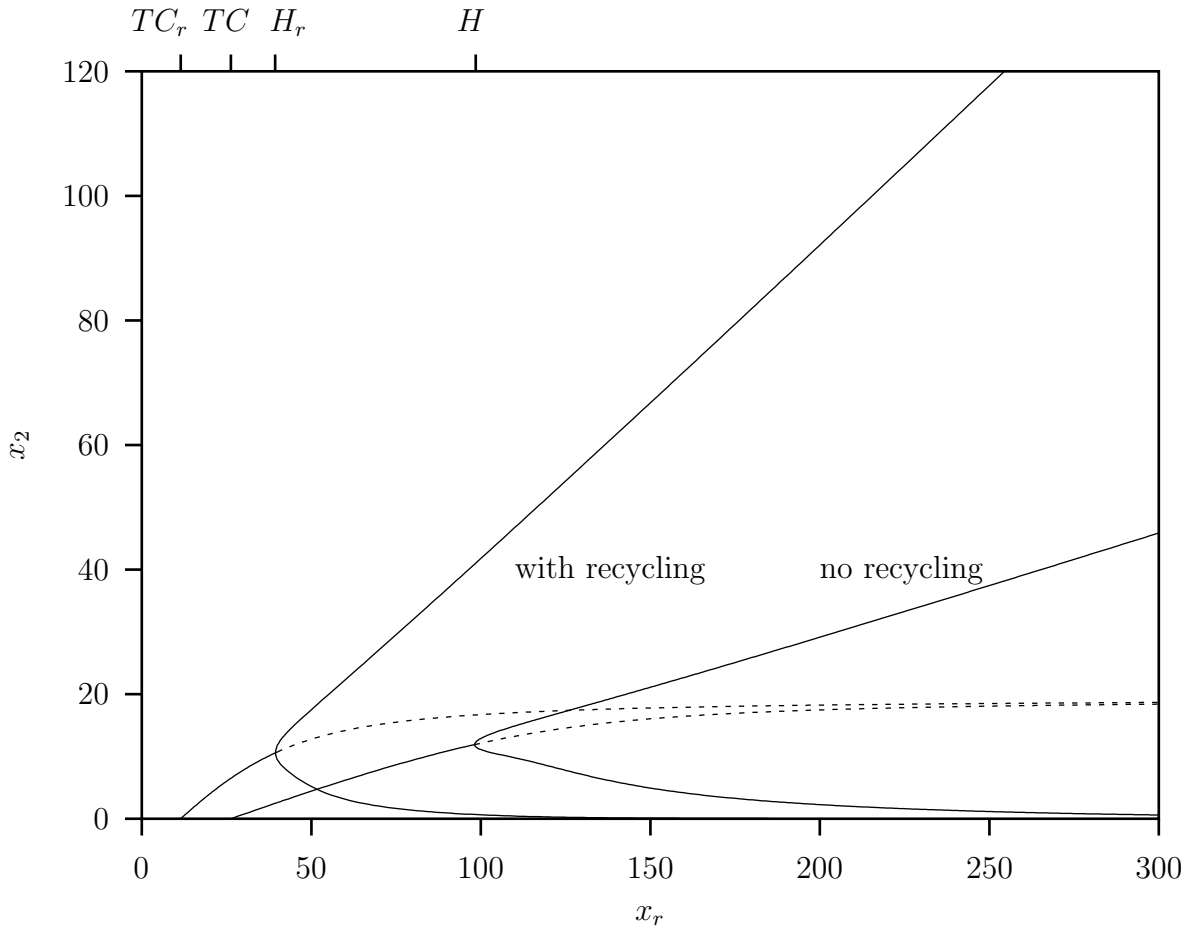


Figure 6:

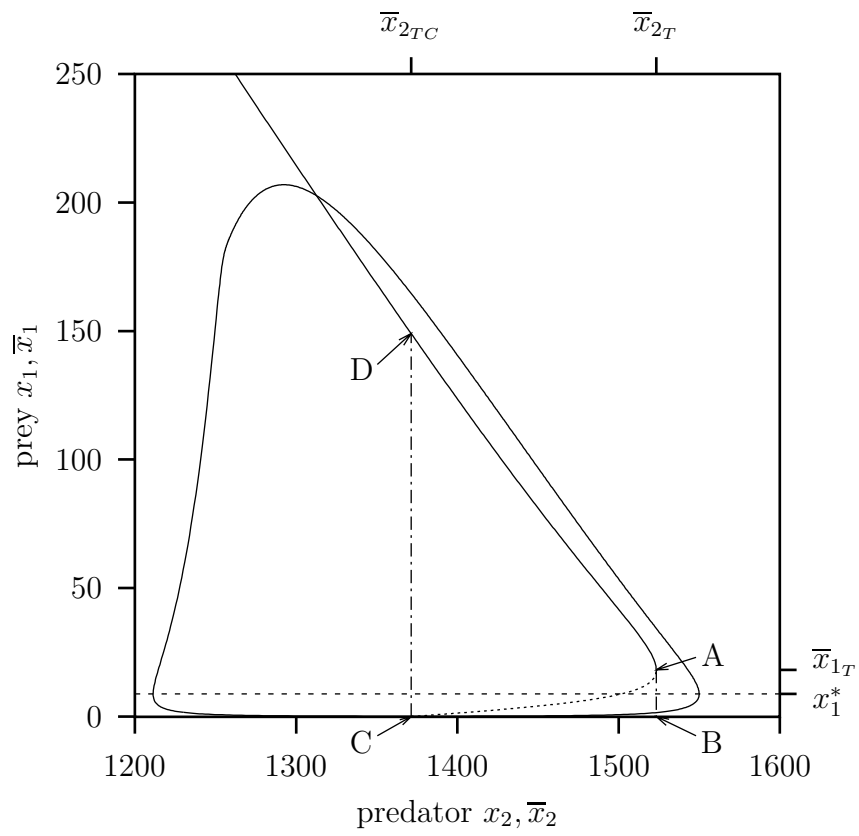


Figure 7: